Department of Physics and Astronomy

University of Heidelberg

Master thesis

in Physics

submitted by

Patrick Fahner

born in Mannheim

September 2015

A study of the decay

$$\Lambda_b^0 \to D^0 p \mu^- \overline{\nu}_\mu X$$

with the LHCb experiment

This Master thesis has been carried out by (Name Surname)

at the

(institute)

under the supervision of

(Frau/Herrn Prof./Priv.-Doz. Name Surname)

(Titel der Masterarbeit - deutsch):

(Abstract in Deutsch, max. 200 Worte. Beispiel: [**?**])
Lorem ipsum dolor sit amet, consectetur adipisici elit, sed eiusmod tempor incidunt ut labore et dolore magna aliqua. Ut enim ad minim veniam, quis nostrud exercitation ullamco laboris nisi ut aliquid ex ea commodi consequat. Quis aute iure reprehenderit in voluptate velit esse cillum dolore eu fugiat nulla pariatur. Excepteur sint obcaecat cupiditat non proident, sunt in culpa qui officia deserunt mollit anim id est laborum.
Duis autem vel eum iriure dolor in hendrerit in vulputate velit esse molestie consequat, vel illum dolore eu feugiat nulla facilisis at vero eros et accumsan et iusto odio dignissim qui blandit praesent luptatum zzril delenit augue duis dolore te feugait nulla facilisi. Lorem ipsum dolor sit amet, consectetuer adipiscing elit, sed diam nonummy nibh euismod tincidunt ut laoreet dolore magna aliquam erat volutpat.
Ut wisi enim ad minim veniam, quis nostrud exerci tation ullamcorper suscipit lobortis nisl ut aliquip ex ea commodo consequat. Duis autem vel eum iriure dolor in hendrerit in vulputate velit esse molestie consequat, vel illum dolore eu feugiat nulla facilisis at vero eros et accumsan et iusto odio dignissim qui blandit praesent luptatum zzril delenit augue duis dolore te feugait nulla facilisi.

(Title of Master thesis - english):

(abstract in english, at most 200 words. Example: [**?**])
Lorem ipsum dolor sit amet, consectetur adipisici elit, sed eiusmod tempor incidunt ut labore et dolore magna aliqua. Ut enim ad minim veniam, quis nostrud exercitation ullamco laboris nisi ut aliquid ex ea commodi consequat. Quis aute iure reprehenderit in voluptate velit esse cillum dolore eu fugiat nulla pariatur. Excepteur sint obcaecat cupiditat non proident, sunt in culpa qui officia deserunt mollit anim id est laborum.
Duis autem vel eum iriure dolor in hendrerit in vulputate velit esse molestie consequat, vel illum dolore eu feugiat nulla facilisis at vero eros et accumsan et iusto odio dignissim qui blandit praesent luptatum zzril delenit augue duis dolore te feugait nulla facilisi. Lorem ipsum dolor sit amet, consectetuer adipiscing elit, sed diam nonummy nibh euismod tincidunt ut laoreet dolore magna aliquam erat volutpat.
Ut wisi enim ad minim veniam, quis nostrud exerci tation ullamcorper suscipit lobortis nisl ut aliquip ex ea commodo consequat. Duis autem vel eum iriure dolor in hendrerit in vulputate velit esse molestie consequat, vel illum dolore eu feugiat nulla facilisis at vero eros et accumsan et iusto odio dignissim qui blandit praesent luptatum zzril delenit augue duis dolore te feugait nulla facilisi.

Contents

1 Introduction

2 The LHCb detector

Most parts of this chapter are taken from [1]

The LHCb experiment is one of the four big experiments, currently running at the Large Hadron Collider (LHC) of the European Organization for Nuclear Research CERN in Geneva, Switzerland. In contrast to the other three experiments – ATLAS and CMS are searching for direct hints of new physics, ALICE investigates the Quark-Gluon-Plasma – LHCb is dedicated to look indirectly for physics beyond the Standard Model (see section **??**) by the study of hadrons containing either a heavy b- or c-quark.

...

The layout of the LHCb detector can be seen in figure 2.1. It is built as a single-arm forward spectrometer. The reason for this choice is, that at LHC energies of $\sqrt{s} = 14\,\text{TeV}$ at the maximum, b- and $\bar{b}$- hadrons are predominantly produced in the forward (or backward) region.

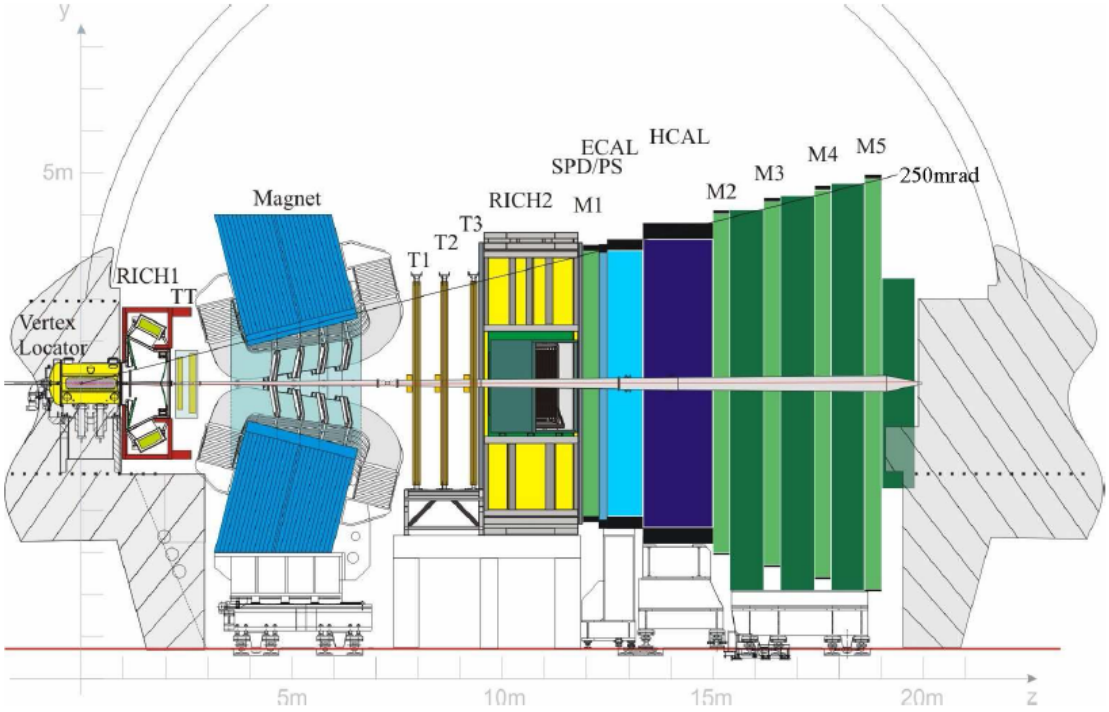

Figure 2.1: The LHCb detector.

2.1 Tracking detectors

Tracking describes the whole procedure to reconstruct the trajectories of the (charged) particles produced in the proton-proton collision. If there's a magnet in use, the particles' charges and momenta can be determined as well. For that purpose, a system of several subdetectors is aligned up- and downstream the dipole magnet, namely the Vertex locator (VELO), the Trigger Tracker (TT) and the Trigger stations (T1-T3) built-up by the Inner Tracker (IT) and the Outer Tracker (OT).

2.1.1 Vertex Locator (VELO)

The VErtex LOcator (VELO) is placed directly around the primary interaction point. Its task is to precisely measure the track coordinates of charged particles and separate the proton-proton interaction point from other vertices, namely either other primary vertices (so called pile-up events) or secondary vertices. The latter ones are typically for b- or c-hadron decays [2] and a good separation and resolution of these vertices is crucial for the LHCb physics programme. As an example serves the measurement of particles' decay length and time for the determination of the rapid $B_s^0 - \overline{B}_s^0$ oscillation frequency [3].

The VELO is built up by silicon modules due to the high particle flux and thus high radiation in the interaction region. It is placed only 7 mm apart from the beam. This is closer than the required aperture of the LHCb beam pipe at injection. Thus, the VELO sensors are made of silicon microstrips shaped as slightly overlapping half-discs. The two halfs can be moved in x- and y-direction to avoid radiation damages unless the beam is stable.

Each module provides a measurement of the r- and ϕ-coordinates. The sensores for these measurements are correspondingly called R- and Φ-sensor, which can be seen in figure 2.2. An overview over the VELO system with its modules is shown in figure 2.3. Around the nominal interaction region, the modules are placed closer to each other. Upstream there are two R sensors dedicated to veto pile-up events. Figure 2.3 furthermore shows the VELO in closed and opened position. With this setup the VELO reaches a track finding efficiency above 98%. Its resolution on vertices is 13 µm in the transverse plane and 71 µm along the beam axis for vertices with 25 tracks. The resolution on the impact parameter is smaller than 35 µm for particles with a transverse momentum larger than 1 GeV [1, 2, 4].

2.1.2 Trigger Tracker / Tracker Turicensis (TT)

The Tracker Turicencis or formerly the Trigger Tracker is located in front of the entrance of the LHCb magnet. It is used for sevaral tasks:

- deliver transverse momentum information for Level-1 trigger,
- reconstruct trajectories of long-lived neutral particles decaying outside the VELO

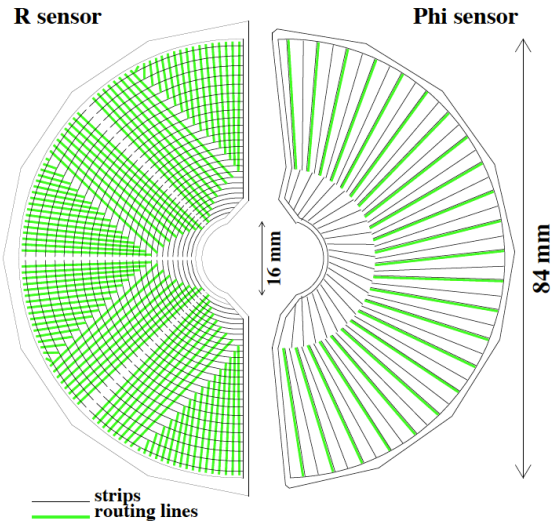

Figure 2.2: Schematic representation of an R and a Φ sensor. The R sensor strips are arranged into four approximately 45° segments and have routing lines perpendicular to the strips. The Φ sensor has two zones with inner and outer strips. The routing lines of the inner strips are orientated parallel to the outer strips. Figure and caption taken from [4].

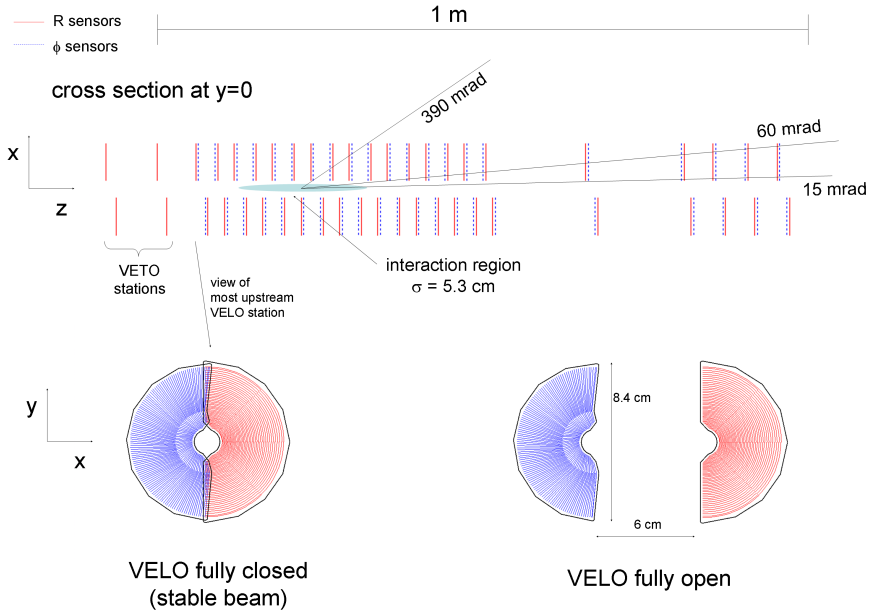

Figure 2.3: Cross section in the (x, z) plane of the VELO silicon sensors, at $y = 0$, with the detector in the fully closed position. The front face of the first modules is also illustrated in both the closed and open positions. The two pile-up veto stations are located upstream of the VELO sensors. Figure and caption taken from [1].

- reconstruct low-momenta particles bent out by the magnet before reaching the station T1-T3.

The TT makes completely use of silicon microstrip detector. It consist of one station made of four planes along the beam axis. The first and the fourth layer have vertical readout strips (x-layer), while the second and third are rotated by an angle $\pm 5°$ to get a high resolution in the bending plane and additional information in y-direction. Between the u and v layer there is a gap of around 30 cm. Figure 2.4 shows schematically the layout of the TT.

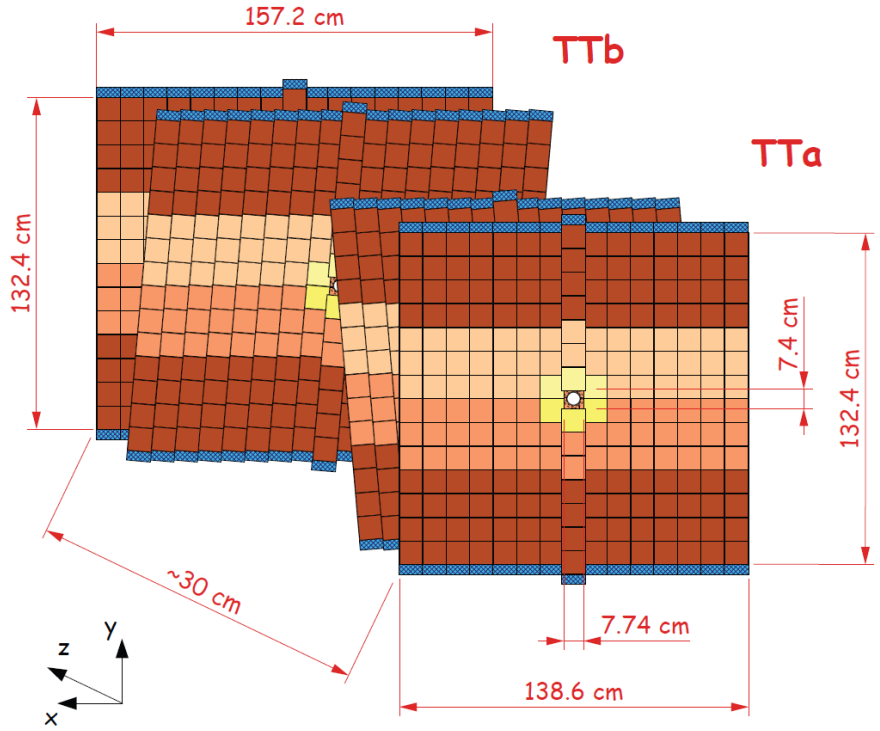

Figure 2.4: Layout of the Tracker Turicensis (TT). Figure taken from [5].

2.1.3 Inner Tracker (IT)

Being a silicon micro-strip detector, the Inner Tracker (IT) uses the same technology as the TT. It builds the inner part of the three tracking stations T1-T3 (see figure 2.1). Each station consists of four boxes as shown in figure 2.5. In each box there are again 4 layers, two vertical and two stereo, analogously to the TT [1, 5].

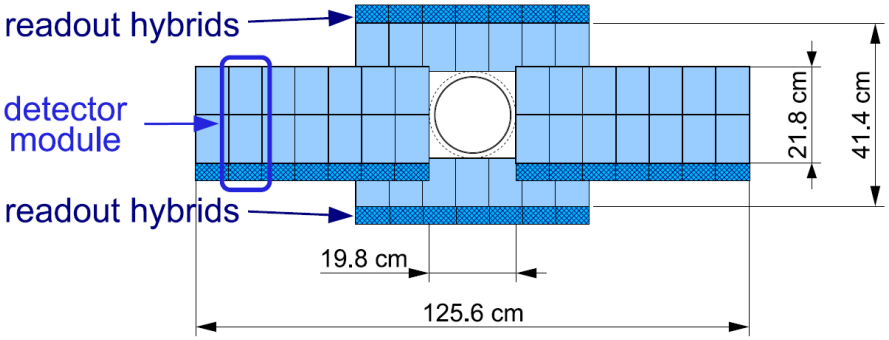

Figure 2.5: Layout of a x detection layer in the second Inner Tracker (IT) station. Figure taken from [1].

2.1.4 Outer Tracker (OT)

2.1.5 Track classification

2.2 Particle identification

2.2.1 Ring Imaging Cherenkoy Detector (RICH)

2.2.2 Calorimeter system

2.2.3 Muon chambers

2.3 Trigger

2.3.1 L0-Trigger

2.3.2 High Level Trigger (HLT)

3 Data reconstruction and selection

The analysis of the decays $\Lambda_b^0 \to D^0 p \mu^- \overline{\nu}_\mu X$ (signal channel) and $\Lambda_b^0 \to \Lambda_c^+ \mu^- \overline{\nu}_\mu$ (normalization channel) requires the reconstruction and selection of possible signal candidates. The term “signal candidates" implies, that a data sample doesn't contain only the desired signal events after reconstruction and selection, but is also polluted by events from different sources, albeit looking like signal. These backgrounds can have several reasons: One possibility is that the final state particles are randomly combined but fulfil all the applied criteria. This kind of background is also known as combinatoric background. There are furthermore the so-called physical backgrounds. With this term one summarises physical decays where one either misidentifies a final state particle or only partially reconstruct an event und thus leading to a wrong interpretation of the decay. As an example for the misidentification consider the decay $\Lambda_b^0 \to D^0 p \pi^-$. If the π^- is now misidentified as a muonthis decay looks exactly like the signal channel of this analysis. Partially reconstructed events play an important role in the normalisation channel $\Lambda_b^0 \to \Lambda_c^+ \mu^- \overline{\nu}_\mu$. There exists also semileptonic Λ_b^0 decays into excited Λ_c^{*+} states, $\Lambda_b^0 \to \Lambda_c^{*+} \mu^- \overline{\nu}_\mu$. Subsequently, these excited Λ_c^{*+} states decay into an Λ_c^+ and additional pions or photons. If one misses these pions and photons the decay looks exactly like $\Lambda_b^0 \to \Lambda_c^+ \mu^- \overline{\nu}_\mu$.

Since such misidentified decays or combinatoric backgrounds distort the measurementof physical quantities, the event reconstruction and above all the selection aims to reduce these backgrounds as much as possible while keeping as much signal as possible. At LHCb, this procedure is done in several steps, described for the present analysis in this chapter, namely the Trigger, the preselction (or stripping) and the offline selection. Nonetheless not every background source can be easily eliminated. The handling of such issues is part of chapter **??**.

3.1 Trigger requirements

Trigger requirements are already applied during data taking to reduce the arising data to a recordable amount. There exists so called trigger lines for different physics purposes. These trigger lines then contain the requirements on the particles' properties.

Due to their large lifetime and their little interaction with matter muons leave a very clean signal in the detector and are the best suited to trigger on. For the $\Lambda_b^0 \to D^0 p \mu^- \overline{\nu}_\mu X$ channel the muon has pass the L0Muon_TOS line at L0 level. TOS is

the abbreviation for Trigger On Signal, i.e. the presence of the signal is sufficient to generate a positive trigger decision [6]. To record an event this line requires that the transverse momentum of at least one muon candidate is larger than 1760 MeV[1]. At Hlt1 two different trigger lines are applied. The Hlt1TrackMuon_TOS line requires the muon candidate to have at least one hit in the VELO and triggers on the track quality.

[1]This requirement changed between 2011 and 2012. For a better readability only the 2012 trigger settings are described here. The 2011 configuration can be found in [?].

4 Normalisation fit

This chapter describes the analysis of the normalisation channel $\Lambda_b^0 \to \Lambda_c^+ \mu^- \overline{\nu}_\mu$ ($\Lambda_c^+ \to pK^-\pi^+$) resulting in the signal yield $N_{\Lambda_c^+}$ for the calculation of $\mathcal{R}$. The method is different to the one in the signal channel $\Lambda_b^0 \to D^0 p\mu^- \overline{\nu}_\mu X$ due to several reasons: The final state particles of the subdecay $\Lambda_c^+ \to pK^-\pi^+$ are all reconstructed. It is thus possible to see a clear Λ_c^+ mass peak as shown in figure 4.1. The small sidebands indicate a small combinatorial background concerning the subdecay $\Lambda_c^+ \to pK^-\pi^+$. Background coming from a random combination of a Λ_c^+ with a muon can be estimated by a look at the WS final states combinations $\Lambda_c^+\mu^+$. Since a Λ_b^0 can't decay into a $\Lambda_c^+\mu^+$ due to charge conservation, this unphysical combination gives a good hint for randomly combined $\Lambda_c^+\mu^-$. The second reason why a different method is chosen compared to the $\Lambda_b^0 \to D^0 p\mu^- \overline{\nu}_\mu X$ channel is the fact that the Λ_b^0 can decay in several excited Λ_c^+ states (in the following denoted as Λ_c^{*+} for any excited Λ_c^+ state). It has been shown in **??** that the $\Lambda_b^0 \to \Lambda_c^+ \mu^- \overline{\nu}_\mu$ data is saturated by the decays $\Lambda_b^0 \to \Lambda_c^*(2595)^+ \mu^- \overline{\nu}_\mu$ and $\Lambda_b^0 \to \Lambda_c^*(2625)^+ \mu^- \overline{\nu}_\mu$. These excited Λ_c^{*+} instantly decay for instance in $\Lambda_c^+\pi^+\pi^-$. If these two pions aren't reconstructed, this decay can't be distinguished by its topology. That's why a different approach for the determination of $N_{\Lambda_c^+}$ has to be chosen. The solution of the latter problem is to fit the corrected $pK^-\pi^+\mu^-$, i.e the visible Λ_b^0 mass. An explanation for this choice and the description of the fit is given in section 4.

4.1 Reduction and handling of backgrounds

This section describes the ways, how different sources of backgrounds are either handled or reduced.

4.1.1 Non Λ_c^+ background

As already mentioned the reconstructed $pK^-\pi^+$ mass delivers a nice peak forming the hadronically decaying Λ_c^+ nicely seen in figure 4.1. Events being outside of this peak can be explained by a random combination of proton, kaon and pion and thus not being decay remnants of the Λ_c^+. Nonetheless there is also a certain amount of this "combinatoric" background in the peak region. It is statistically eliminated by a sideband subtraction (see section **??**). As signal band the invariant $pK^-\pi^+$ masses in the range $\mathrm{M}(pK^-\pi^+) \in [2260, 2320]$ MeV are chosen. The background bands are $\mathrm{M}(pK^-\pi^+) \in [2225, 2260]$ MeV or $\mathrm{M}(pK^-\pi^+) \in [2320, 2345]$ MeV.

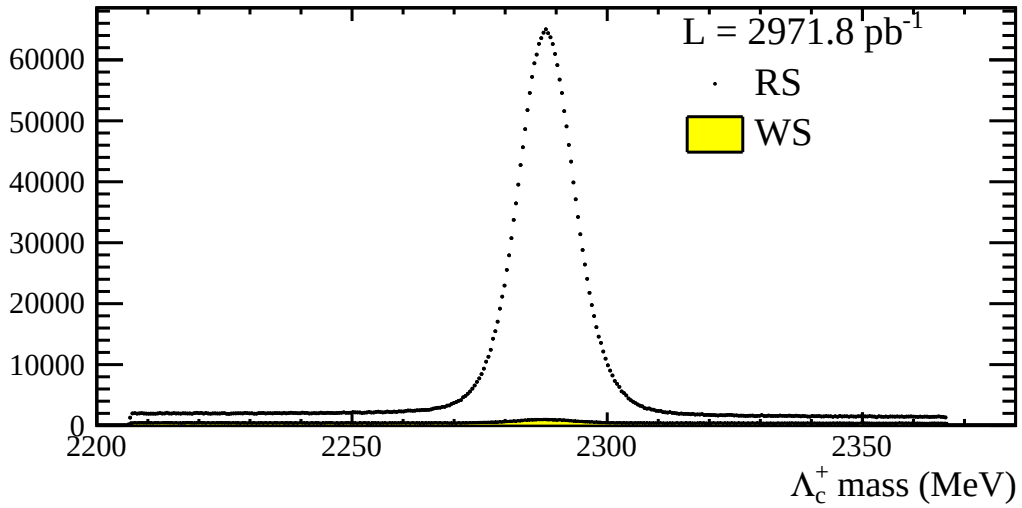

Figure 4.1: Plot of the invariant $pK^-\pi^+$ mass. A clear mass peak identified as the Λ_c^+ can be seen. The yellow shaded area shows events with the WS combination $\Lambda_c^+\mu^+$.

4.1.2 Random combinations of Λ_c^+ and μ^-

The next possible source of backgrounds are random combinations of Λ_c^+ and μ^-. Due to the semileptonic decay $\Lambda_b^0 \to \Lambda_c^+\mu^-\overline{\nu}_\mu$ and hence the missing neutrino $\overline{\nu}_\mu$ it is not possible to use a sidebandsubtraction on the invariant $pK^-\pi^+\mu^-$ ($\Lambda_c^+\mu^-$) mass. Thus, wrong sign (WS) events, i.e. "unphysical" events with a $\Lambda_c^+\mu^+$ in the final state as explained above are used to estimate the amount of random $\Lambda_c^+\mu^-$ background. While trying to perform the final fit later (see sec. 4.2) it turns out, that the number of WS events is too small that the fit is sensitive to it. As a consequence it is assumed that the shape and the number of the WS events are equal to the shape and number of random $\Lambda_c^+\mu^-$ combinations. Finally, the WS events are subtracted from the "right sign" (RS) events to eliminate this source of backgrounds.

4.1.3 Peaking backgrounds

The third source of backgrounds is peaking background from partially reconstructed decays. In this case the data is saturated by the decays $\Lambda_b^0 \to \Lambda_c^*(2595)^+\mu^-\overline{\nu}_\mu$ and $\Lambda_b^0 \to \Lambda_c^*(2625)^+\mu^-\overline{\nu}_\mu$ [7]. The Λ_c^{*+} subsequently decay in a Λ_c^+ and an untracked neutral remnant, e.g. π^0, $\pi^+\pi^-$. Since this decay happens instantly it looks the same as $\Lambda_c^+ \to pK^-\pi^+$ in the detector. The solution is to fit the corrected $pK^-\pi^+\mu^-$ (alias the visible Λ_b^0) mass. A property of the corrected mass is that if the only missing particle is a massless, then the corrected mass should peak around the real mass of the mother particle, here the Λ_b^0. If there are additionally more missing, but massive particles then this peak should be shifted to lower masses. It is thus expected that

the corrected $pK^-\pi^+\mu^-$ mass distributions look different for the semileptonic Λ_b^0 decays into a Λ_c^+, $\Lambda_c^*(2595)^+$ and $\Lambda_c^*(2625)^+$. A fit of the corrected mass should also be able to distinguish between those components.

4.2 Fit of the $pK^-\pi^+\mu^-$ corrected mass

Having read the previous sections it should be clear, why the corrected $pK^-\pi^+\mu^-$ mass is used for the determination of $N_{\Lambda_c^+}$, the $\Lambda_b^0 \to \Lambda_c^+\mu^-\overline{\nu}_\mu$ signal yield. Nonetheless it should be verified, that the corrected $pK^-\pi^+\mu^-$ mass is an appropriate variable. Therefore simulations for the different components, $\Lambda_b^0 \to \Lambda_c^+\mu^-\overline{\nu}_\mu$, $\Lambda_b^0 \to \Lambda_c^*(2595)^+\mu^-\overline{\nu}_\mu$ and $\Lambda_b^0 \to \Lambda_c^*(2625)^+\mu^-\overline{\nu}_\mu$ are used to compare their corrected $pK^-\pi^+\mu^-$ mass shapes.

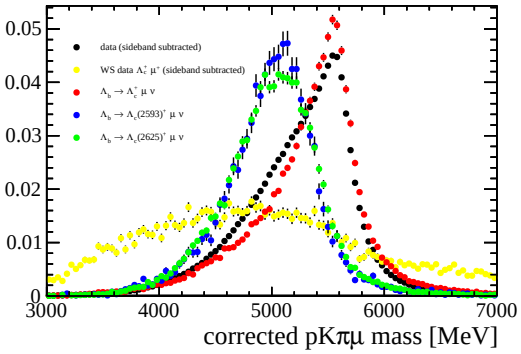

Figure 4.2: Comparison of the $pK^-\pi^+\mu^-$ corrected mass for the semileptonic Λ_b^0 decays via Λ_c^+, $\Lambda_c^*(2593)^+$ and $\Lambda_c^*(2625)^+$ gained from simulation. The black points show the sideband subtracted data distribution. The shape of combinatorial $\Lambda_c^+\mu^-$ background (WS events) is shown in yellow.

From figure 4.2 one can draw the following conclusions:

- The corrected $pK^-\pi^+\mu^-$ mass indeed looks different for Λ_c^+ and Λ_c^{*+} channels.
- It is not possible to distinguish between the $\Lambda_c^*(2595)^+$ and $\Lambda_c^*(2625)^+$ as their shapes are too similar.

The latter conclusion isn't really a problem since the only result of interest is the $\Lambda_b^0 \to \Lambda_c^+\mu^-\overline{\nu}_\mu$ signal yield. A distinction among the excited states isn't needed. In the fit there will be just a component for both final states. Having these in mind, the fit procedure is done as follows:

1. The data is subtracted by the $pK^-\pi^+$ (i.e. Λ_c^+) mass bands.
2. The corrected $pK^-\pi^+\mu^-$ mass distribution is subtracted by the WS events' distribution.

3. A fit of the $pK^-\pi^+\mu^-$ mass is performed using the Beeston-Barlow method (see sec. **??**) to account for uncertainties in the MC corrected mass templates. The fitted components are the Λ_c^+ signal yield and one for both excited Λ_c^{*+} channels.

4. For the plotting (see fig. 4.3 and a better comparison the WS component is added again.

The results can be seen in figure 4.3 and table 4.1. The $\Lambda_b^0 \to \Lambda_c^+ \mu^- \overline{\nu}_\mu$ signal yield $N_{\Lambda_c^+}$, required for the determination of $\mathcal{R}$ is:

$$N_{\Lambda_c^+} = (1.5837 \pm 0.0098) \cdot 10^6$$

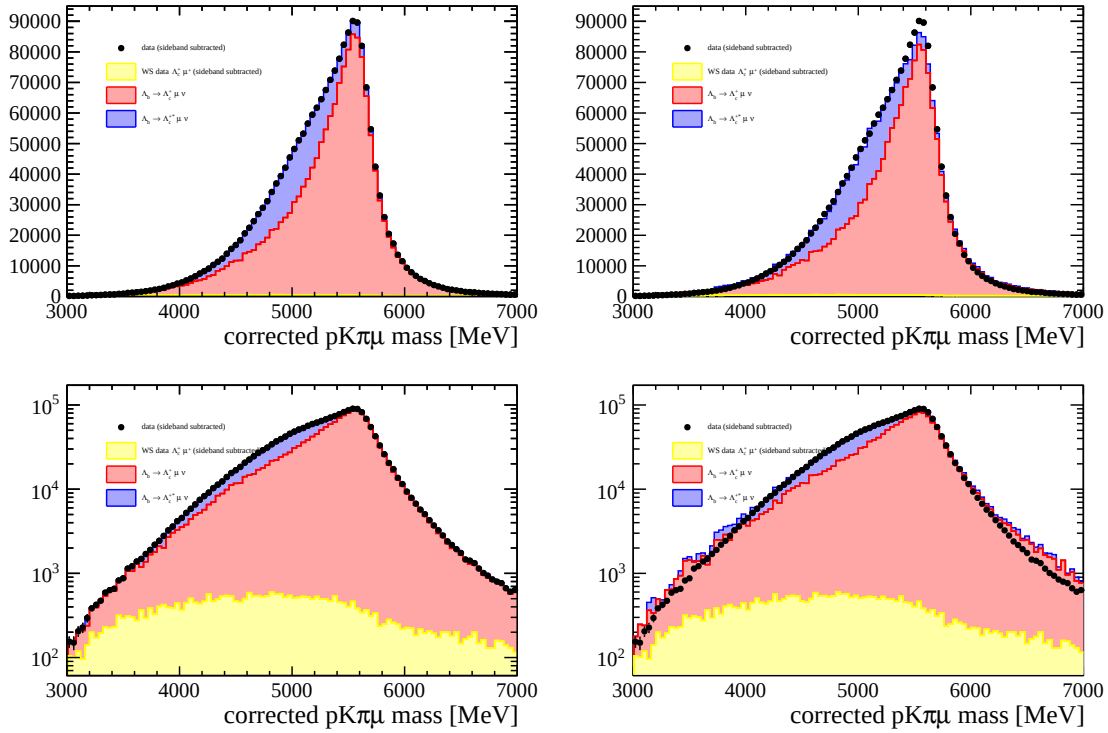

Figure 4.3: Fit to the $pK^-\pi^+\mu^-$ corrected mass for the determination of the $\Lambda_b^0 \to \Lambda_c^+ \mu^- \overline{\nu}_\mu$ signal yield. The left plot shows the fitresult with the Beeston-Barlow adjusted templates, the right one the bare templates without any modification. The top row shows the result on a linear, the bottom row on logarithmic scale.

Table 4.1: Results of the Λ_c^+ corrected mass fit.

Variable	Value
Λ_c^+ candidates $N_{\Lambda_c^+}$	$(1.58 \pm 0.01) \cdot 10^6$
excited Λ_c^{*+} candidates	$(3.85 \pm 0.09) \cdot 10^5$
combinatoric background	$(3.41 \pm 0.03) \cdot 10^4$

Part I

Appendix

A Lists

List of Figures

List of Tables

Bibliography

[1] LHCb collaboration, A. A. Alves Jr. *et al.*, *The LHCb detector at the LHC*, JINST **3** (2008) S08005.

[2] LHCb Collaboration, *LHCb VELO (VErtex LOcator): Technical Design Report*, Technical Design Report LHCb, CERN, Geneva, 2001.

[3] LHCb, R. Aaij *et al.*, *Precision measurement of the B_s^0-$\bar{B}_s^0$ oscillation frequency with the decay $B_s^0 \to D_s^- \pi^+$*, New J. Phys. **15** (2013) 053021, arXiv:1304.4741.

[4] R. Aaij *et al.*, *Performance of the LHCb Vertex Locator*, JINST **9** (2014) 09007, arXiv:1405.7808.

[5] LHCb Silicon Tracker Group, J. Luisier, *Performance of LHCb Silicon Tracker Detector in the LHC*, Phys. Procedia **37** (2012) 851.

[6] S. Tolk, J. Albrecht, F. Dettori, and A. Pellegrino, *Data driven trigger efficiency determination at LHCb*, Tech. Rep. LHCb-PUB-2014-039. CERN-LHCb-PUB-2014-039, CERN, Geneva, May, 2014.

[7] LHCb, R. Aaij *et al.*, *Determination of the quark coupling strength $|V\_ub|$ using baryonic decays*, arXiv:1504.0156.

Erklärung:

Ich versichere, dass ich diese Arbeit selbstständig verfasst habe und keine anderen als die angegebenen Quellen und Hilfsmittel benutzt habe.

Heidelberg, den (Datum) .....